

RESEARCH

Open Access



# Performance and design analyses of various configurations of dew point evaporative cooling-based desiccant air-conditioning (DAC) systems for hot and humid conditions

Marco Lao<sup>1\*</sup>, Jie Lin<sup>2</sup>, František Mikšík<sup>1,3</sup>, Kyaw Thu<sup>1,3</sup> and Takahiko Miyazaki<sup>1,3</sup>

## Abstract

Thermally driven desiccant- and evaporative cooling-based technologies are promising greener and cheaper alternatives to compressor-based systems due to the separate handling of latent and sensible loads. Desiccant air-conditioning (DAC) systems comprise a desiccant dehumidifier, a sensible cooling unit, a heat source for regeneration, and a heat recovery unit. These components of a DAC system can be arranged in various ways to give different configurations with varying advantages and disadvantages. In this study, five configurations of thermally driven desiccant dehumidifier- and dew point evaporative cooling (DPEC)-based DAC systems were investigated. Seven evaluation criteria namely regeneration temperature, desiccant moisture removal capacity, COP<sub>t</sub>, DPEC L/H, heat exchanger UA, system size, and fan power requirement were employed. Results show that the standard cycle in ventilation mode offers the highest COP<sub>t</sub> despite having the highest regeneration temperature. Recirculation of the return room air can operate at a significantly lower regeneration temperature at the expense of larger equipment size and much lower COP<sub>t</sub>. DAC with an internally cooled dehumidification can operate at low regeneration temperature at the expense of higher fan power and slightly lower COP<sub>t</sub>. Dividing the dehumidification process into two stages can offer operation at moderately lower regeneration temperature without severely affecting the other criteria. This study can serve as a guide for the selection of an appropriate DAC configuration for space cooling depending on the objective criteria and the resources available.

**Keywords:** Desiccant air-conditioning, Dew point evaporative cooling, Space cooling, Regeneration temperature, Waste heat, Thermal comfort

## 1 Introduction

Space cooling consumes a huge fraction of electricity end use in tropical countries. In the Philippines, mean maximum dry bulb temperature and specific humidity range from 30.2 to 23.0 g/kg dry air (83.8% RH) in the rainy months to 33.4 °C and 24.9 g/kg dry air (75.5%

RH) in summer which is far outside the thermal comfort zone recommended by ASHRAE 55 [1]. In 2011, 31.1% of electricity end use in the residential sector was used for space cooling and air-conditioning (AC) [2]. In the ASEAN region, AC ownership is expected to grow in the coming decades from the current average of 10% as the region continues to industrialize and economies progress [3, 4]. Thermally driven desiccant- and evaporative cooling-based technologies are promising greener and cheaper alternatives to compressor-based systems due to the separate handling of latent and sensible loads. These systems utilize thermal energy as the

\*Correspondence: marco\_lao@yahoo.com

<sup>1</sup> Department of Energy and Environmental Engineering, Interdisciplinary Graduate School of Engineering Sciences, Kyushu University, 6-1, Kasuga-koen, Kasuga, Fukuoka 816-8580, Japan  
Full list of author information is available at the end of the article

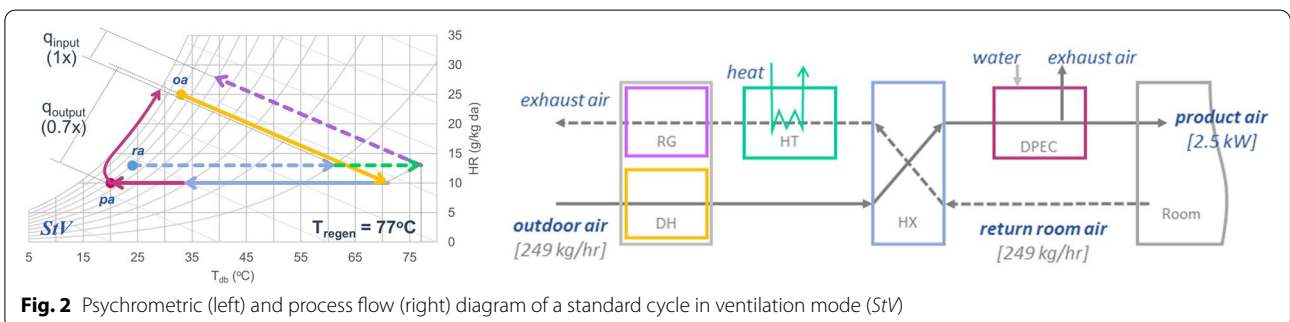
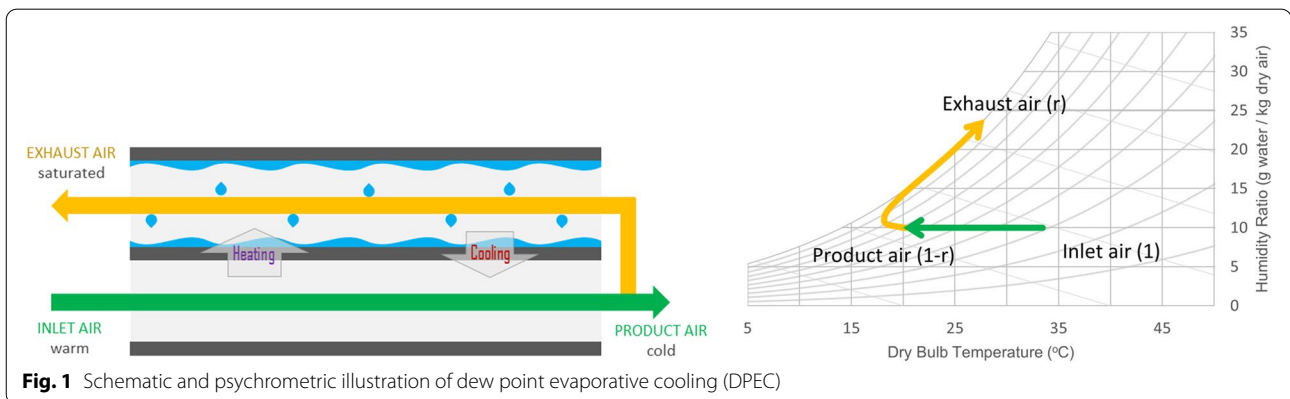
primary energy source while using minimal electricity to drive the flow of air. As such, these systems can reduce the reliance on fossil fuel-derived electricity. In addition, when operated using solar heat, these systems can run at significantly reduced operating costs and appreciably reduce the electricity use during peak hours, thereby lessening the strain to power producers.

Desiccant air-conditioning (DAC) systems, in general, consist of a desiccant dehumidifier for latent heat reduction, a cooling unit for sensible heat reduction, a heat source for desiccant regeneration, and a heat exchanger for heat recovery. While several studies have been performed on DACs based on direct evaporative cooling (DEC) [5–9], DACs based on dew point evaporative cooling (DPEC) have only gained greater interest recently [10–13]. Dew point evaporative cooling, also known as Maisotsenko cycle, regenerative evaporative cooling, or wet surface heat exchange, is an indirect evaporative cooling process capable of cooling the air to its dew point temperature which is lower than the wet bulb temperature limit of conventional DEC. In DPEC, a single stream of air flows sequentially through the dry and wet channels (Fig. 1) where the evaporative cooling in the wet channel cools the air in the dry channel, and the warmer air in the dry channel provides

additional driving force to the wet channel for evaporation [14–16].

DAC systems can be arranged in various configurations for air-conditioning applications. The most common configuration is the standard cycle in ventilation mode, also known as open cycle, as shown in Fig. 2. Due to the exothermic nature of adsorption, the temperature increases as humidity decreases during desiccant dehumidification. The regeneration temperature required to desorb the moisture from the desiccant is defined by the temperature of the regeneration air at the same relative humidity. As such, in order to decrease the humidity level of humid air to comfortable levels, high regeneration temperature is usually necessary, thereby limiting the application of the open cycle configuration.

In recent years, several efforts have been made to reduce the regeneration temperature of desiccant dehumidification as well as to improve the adsorption capacity of the desiccant to mimic the ideal isothermal route by performing dehumidification with internal cooling or multistage dehumidification with interstage cooling. Desiccant wheels with internal cooling mechanism using cooling water have been shown to improve the dehumidification performance by 45–53% [17] and 48% [18]. Improved dehumidification performance was achieved



when the temperature difference between the cooling water and inlet air was increased, when the regeneration temperature was increased, and when the inlet air humidity is high [19]. Due to the challenges involved with the removal of adsorption heat in rotary-based desiccant wheels, desiccant-coated heat exchangers (DCHE) were proposed and investigated as an alternative design to realize isothermal dehumidification (Ge et al., 2013; Ucok et al., 2018; Vivekh et al., 2018). The fins of the pipes of a heat exchanger are impregnated with desiccant which dehumidifies the air, whereas adsorption heat is removed by the cooling water flowing in the tubes, thereby increasing the heat transfer rate.

Elzahzby and co-authors [20] numerically investigated a DEC-based DAC system with two stages of dehumidification performed in series and two-stage regeneration performed in parallel using a desiccant wheel dehumidification area to regeneration area ratio of 11:2. To compensate for the lower regeneration area and parallel operation of regeneration, a much higher regeneration temperature was employed to expedite desorption. Nevertheless, a COPt of 1.25 was obtained for a cooling capacity of 2.6 kW. Ge and co-authors [21] experimentally studied a similar DEC-based DAC system with two-stage series dehumidification and two parallel regeneration using a process air to regeneration air mass flux ratio of 2.43:1. As such, higher regeneration temperature was used. Moisture removal by the desiccant displayed increasing trend as regeneration temperature was increased, whereas COPt was negatively affected. Huan and Niu [22] numerically studied a two-stage DEC-based DAC system wherein both dehumidification and regeneration were performed in series. A COPt of 0.979 was realized at a regeneration temperature of 60 °C. Gadalla and Saghafifar [11] studied three configurations of DPEC-based DAC systems using three DPECs which served as either interstage cooler or final sensible cooler. Outdoor air was conditioned from 40 °C and 0.015 kg/kg da to roughly 13 °C and 0.0075 kg/kg da using a regeneration temperature

of 60 °C. An average COPt of 1.77 was achieved using a solar heater as the heat source.

An alternative means to condition air at much lower regeneration temperature is by recirculating the colder and drier return room air as the process air and repeatedly decreasing its latent and sensible heat load. Bourdoukan and co-workers [23] compared the performance of DEC-based DAC system for a ventilation cycle and recirculation cycle at the same regeneration temperature. The heating requirement for regeneration is higher for recirculation cycle than the ventilation cycle. In addition, ventilation cycle was found to be more sensitive to the inlet air conditions than recirculation cycle.

DAC systems can be arranged and operated in countless number of ways depending on the number of components. These arrangements have their own advantages and disadvantages depending on the outdoor air conditions and objective criteria. This study aims to consolidate five general configurations of DAC systems based on DPEC for hot and humid conditions, namely standard cycle in ventilation mode (*StV*) aka open cycle, standard cycle in recirculation mode (*StR*), internally cooled dehumidification (*ICD*), 2-stage dehumidification without interstage cooling (*2SD*), and 2-stage dehumidification with interstage cooling (*2SD-IC*) as shown in Figs. 2, 3, 4, 5 and 6, respectively. These configurations were evaluated in terms of seven criteria, namely regeneration temperature, moisture removal capacity of the desiccant, thermal COP, DPEC L/H, heat exchanger UA, system size, and fan power requirement. This work can serve as guide for the selection of an appropriate configuration depending on the situation and desired objectives.

## 2 Methodology

### 2.1 DAC configurations and operating conditions

The operating conditions employed in this study are listed in Table 1. For humidity control, rotary honeycomb desiccant wheel with RD-type silica gel operating in 1:1 area ratio for adsorption and desorption modes

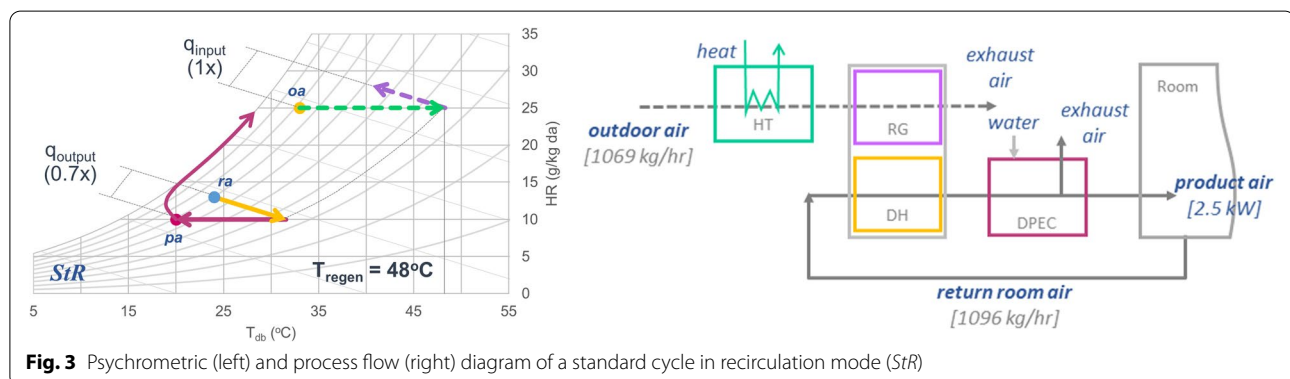


**Fig. 3** Psychrometric (left) and process flow (right) diagram of a standard cycle in recirculation mode (*StR*)

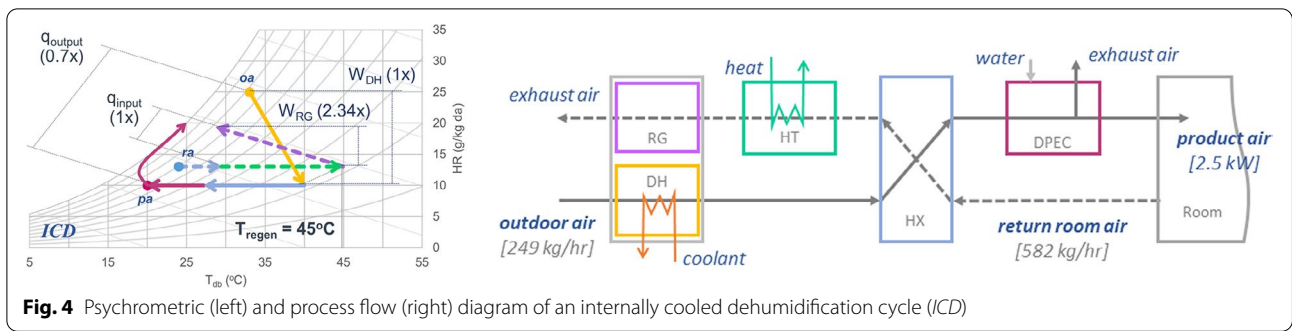


**Fig. 4** Psychrometric (left) and process flow (right) diagram of an internally cooled dehumidification cycle (ICD)

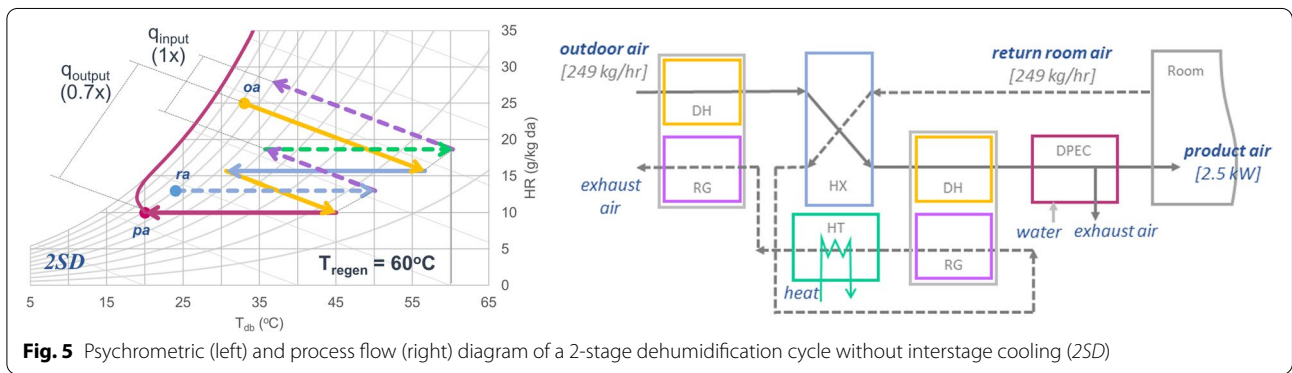


**Fig. 5** Psychrometric (left) and process flow (right) diagram of a 2-stage dehumidification cycle without interstage cooling (2SD)

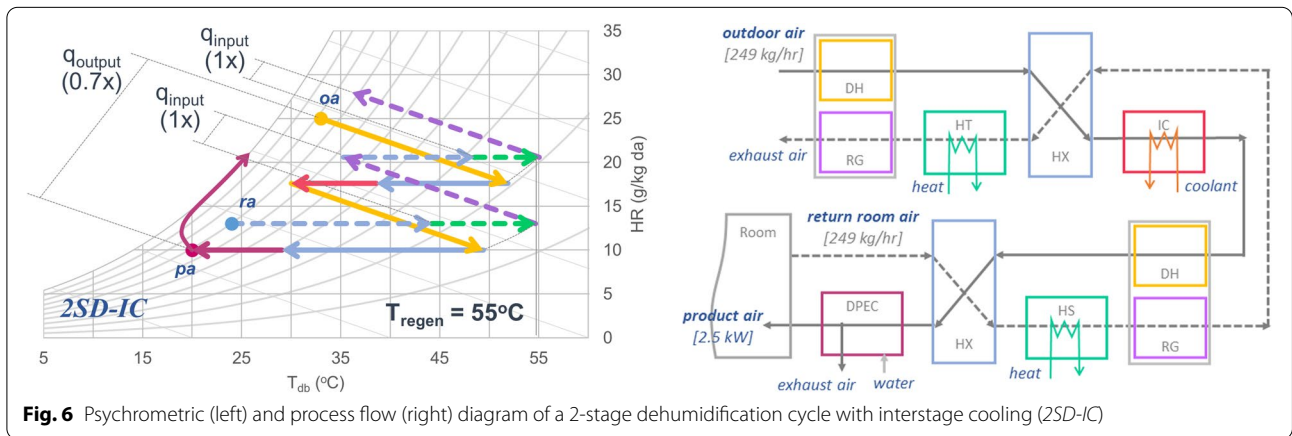


**Fig. 6** Psychrometric (left) and process flow (right) diagram of a 2-stage dehumidification cycle with interstage cooling (2SD-IC)

was considered. For sensible cooling, a counterflow dew point evaporative cooler was used. For heat recovery, a counterflow plate-and-fin-type heat exchanger was adopted. Table 2 shows the relevant design parameters of the DAC components.

In *StV* (Fig. 2), fresh outdoor air is dehumidified with concurrent increase in temperature. The high-temperature dehumidified air is pre-cooled via heat exchange with the regeneration air, which is the room return air, after which is sensibly cooled by the DPEC. In *StR* (Fig. 3), the return room air is used as the inlet to the dehumidifier

after which is fed directly to the DPEC for sensible cooling. Due to recirculation of the cold and dry room air as the process air, the set point can be achieved even at lower regeneration temperature at the expense of lower specific enthalpy reduction. As a compensation, higher air flowrates are necessary to meet the required cooling capacity. Configuration *ICD* (Fig. 4) works similar to *StV* with the addition of a heat rejection mechanism during dehumidification to provide the same specific humidity reduction even at lower regeneration temperatures. However, at lower regeneration temperature, the specific

**Table 1** DAC operating parameters and air conditions

Operating parameter	Value	Configuration	Specific enthalpy reduction (kJ/kg da)	Process air flowrate (kg/h)	Regeneration air flow rate (kg/h)	Regeneration temperature (°C)
DAC cooling capacity, kW	2.5	<i>StV</i>	51.7	249	249	77.1
Product air velocity, m/s	0.7	<i>StR</i>	11.7	1096	1096	48.3
DPEC working ratio	0.3	<i>ICD</i>	51.7	249	582	44.9
Outdoor air temperature °C	33	<i>2SD</i>	51.7	249	249	60.3
Outdoor air humidity, kg/kg da	0.025	<i>2SD-IC</i>	51.7	249	249	55.0
Product air temperature °C	20					
Product air humidity, kg/kg da	0.010					
Return room air temperature, °C	24					
Return room air humidity, kg/kg da	0.013					

**Table 2** DAC component channel parameters and pressure drop coefficients

Equipment	Channel shape	Channel height, m	Channel width, m	<i>fRe</i>	Minor loss component	Loss coefficient, $\zeta$
Desiccant wheel	Sinusoidal	0.00175	0.0035	52.96 [24]	Sudden contraction	0.5
DPEC <sup>a</sup>	Rectangular	0.004	0.040	84.70 [25]	Sudden expansion	1.0
Heat exchanger	Rectangular	0.004	0.006	58.86 [25]	180° diversion	1.1

<sup>a</sup> Channel dimensions are the same for both dry and wet channels

moisture holding capacity of the regeneration air is lower due to its higher relative humidity and hence must operate at higher air flowrates to desorb the same amount of adsorbed moisture. In *2SD* (Fig. 5), dehumidification is divided into two stages, using the same total desiccant length and same set of equipment as *StV*, to allow the same specific humidity reduction using a moderately lower regeneration temperature. The dehumidified air exiting the first stage is pre-cooled via heat exchange with the return room air prior to the second-stage dehumidification. The dehumidified air from the second-stage desiccant unit is then directly fed to the DPEC at much higher temperature. In this configuration, dehumidification is divided such that the outlet temperature in the first stage is high enough to serve as the heat source for the regeneration of the desiccant in the second stage. As such, the first-stage desiccant unit does more dehumidification than the second. In configuration *2SD-IC* (Fig. 6), dehumidification is performed in two stages with an additional intercooler to further pre-cool the air entering the second stage. This increases the dehumidification capacity of the second desiccant unit, thereby reducing the dehumidification load in the first stage. Due to the more even distribution of dehumidification between the two stages, a much lower temperature can be used for regeneration. Heat recovery is performed after the first

and second stages of dehumidification to pre-cool the dehumidified air as well as pre-heat the regeneration air.

## 2.2 Psychrometric and performance analysis

Process and regeneration air conditions were analyzed using psychrometric relationships and illustrated in a psychrometric chart. Adiabatic dehumidification and regeneration were assumed to follow the constant enthalpy line. Regeneration temperature is depicted to be the temperature of the regeneration air at the same relative humidity as that of the dehumidified air. Likewise, the outlet relative humidity after regeneration cannot exceed that of the supply air.

The specific enthalpy of air was calculated as a function of temperature and humidity ratio. The mass flowrate of the process air,  $m_p$ , is calculated based on the 2.5 kW cooling capacity ( $Q_{\text{output}}$ ) and the specific enthalpy difference between the supply air and the product air. The mass flowrate of the regeneration airstream is calculated from the moisture balance between dehumidification and regeneration. Heating load ( $Q_{\text{input}}$ ) is calculated as the difference between the enthalpy before and after heating. Thermal COP was calculated as the cooling capacity divided by the total heat input. Additional cooling related to internal cooling for *ICD* and interstage cooling for *2SD-IC* was disregarded in COPt calculation on the

assumption that the coolant is sourced from the ambient and is free.

$$h = C_{p,a}T + (C_{p,v}T + h_{vap})W \quad (1)$$

$$m_p = \frac{Q_{output}}{(h_{DH,in} - h_{DPEC,out})} \quad (2)$$

$$m_r = \frac{m_p(W_{DH,in} - W_{DH,out})}{(W_{RG,out} - W_{RG,in})} \quad (3)$$

$$Q_{input} = m_r(h_{HT,out} + h_{HT,in}) \quad (4)$$

$$COP_t = \frac{Q_{output}}{Q_{input}} \quad (5)$$

$h_{vap}$  is the latent heat of vaporization of water at 0 °C (2501 kJ/kg), whereas  $C_{p,a} = 1.006$  kJ/kg-K and  $C_{p,w} = 1.805$  kJ/kg-K. Outlet temperatures during heat exchange were calculated via the NTU method at 80% effectiveness. Likewise, the heat exchanger UA, which represents the required heat transfer area given a certain overall heat transfer coefficient, was also derived to compare the design requirement to achieve 80% heat recovery.

### 2.3 Component design parameters

During dehumidification, sorption occurs only at a certain span of the entire sorbent bed length also known as the mass transfer zone or breakthrough curve length. This length, which depends of rates of heat and mass transfer, prescribes the minimum length of the bed which will give the desired minimum humidity of the air. At the onset of dehumidification, the breakthrough curve commences at the entrance region and slowly moves toward the flow direction as the sorbent reaches its maximum adsorption capacity. Increasing the bed length beyond the breakthrough curve length does not affect the outlet air humidity but rather allows for a longer dehumidification period before switching to regeneration while also increasing pressure drop and material cost. Customarily, the desiccant bed length is designed to be slightly longer than the breakthrough curve length under ordinary operating conditions but not overly long to extensively increase pressure loss and material cost. On the assumption that the minimum humidity achievable mainly depends on the relative humidity of the regeneration air,

and that the desiccant wheel operates at their optimum rotational speed, a fixed desiccant bed length of 0.3 m was used per 0.015 kg/kg da humidity reduction for all configurations. For multistage systems, the bed length was divided relative to the humidity reduction per stage. For the system operating in recirculation mode, the desiccant length was calculated based on humidity reduction at the onset of operation which is greater than when at steady state. The length of the DPEC was calculated by multiplying DPEC L/H (see Section 2.5) to the channel height. For the plate-fin heat exchanger, its length was calculated as follows for laminar flow [25]:

$$L_{HX} = \frac{PrRed_hNTU}{4Nu} \quad (6)$$

$$Nu = 7.541(1 - 2.61\alpha + 4.97\alpha^2 - 5.119\alpha^3 + 2.702\alpha^4 - 0.548\alpha^5) \quad (7)$$

where  $\alpha$  is the ratio of the shorter side to the longer side of the channel. The flow cross-sectional areas of the DAC components were calculated as a function of the air volumetric flowrate, derived using the average air density per process.

### 2.4 Moisture removal capacity

RD silica gel was used as the desiccant in the study. The effective moisture removal capacity (MRC) of the desiccant dehumidifier was calculated as shown in Eq. 8. Adsorption uptake for RD silica gel was evaluated according to the Dubinin-Astakhov model in Eq. 9 [26]:

$$MAC = \frac{\sum m_{ads,i}(w_{inlet,i} - w_{regen,i})}{\sum m_{ads,i}} \quad (8)$$

$$w = w_o \exp \left\{ - \left( \frac{RT_s}{E} \ln \frac{P_s}{P_v} \right)^n \right\} \quad (9)$$

where  $w_o = 0.48$  kg H<sub>2</sub>O/kg adsorbent,  $R = 8.314$  J/mol-K,  $E = 3030 + 192RH^{-\frac{1}{1.3}}$  J/mol, and  $n = 1.6$ . The mass of the desiccant was calculated from the desiccant wheel design parameters and a desiccant thickness of 0.0002 m.

### 2.5 DPEC L/H

The ratio of the DPEC length to its channel height was used as the criteria to evaluate the dimensionless length required for the DPEC inlet air to be cooled to the desired product air temperature. This parameter was estimated using the following empirical correlation as developed

by Lin et al. [27] which describes the relationship among DPEC geometric parameters, operating parameters, and supply and outlet air conditions.

$$\frac{T_p - T_{in}}{T_{dp,in} - T_{in}} = 97.537 \frac{\left(\frac{\delta}{H_{1/2}}\right)^{0.0941} \left\{ \frac{h_{vap} D_{wa} (\rho_{vs,ex} - \rho_{v,in})}{k_w (T_{dp,in} - T_{in})} \right\}^{1.4606} (1 - 0.20245r^{-0.52818})}{\left(\frac{uz_{DPEC}}{v}\right)^{0.48} \left(\frac{z_{DPEC,1/2}}{L_{DPEC}}\right)^{0.401}} \quad (10)$$

For the determination of  $\rho_{vs,ex}$ , mass and energy balances were performed assuming a product air temperature at the dew point and employing a fixed working ratio of 0.5 [27].

## 2.6 Fan power

The minimum fan power requirement was calculated based on the pressure drop across all the DAC components according to the following equations [28]:

$$FP = \frac{\Delta PV \eta_2}{\eta_0 \eta_1} \quad (11)$$

$$\Delta P = f \frac{L}{d_h} \frac{\rho u^2}{2} + \sum \zeta \frac{\rho u^2}{2} \quad (12)$$

where  $\eta_0$ ,  $\eta_1$ , and  $\eta_2$  are the fan internal efficiency, mechanical efficiency, and motor capacity coefficient with values of 0.75, 0.90, and 1.1, respectively.  $fRe$ , from which the friction factor,  $f$ , was derived, and the loss coefficient,  $\zeta$ , is listed in Table 2 [28].

## 3 Results and discussion

### 3.1 General features

The general operating parameters for the five DAC configurations are summarized in Table 1. For a continuous and balanced operation, the moisture adsorbed by the desiccant during dehumidification must be equally removed during regeneration. For a 1:1 desiccant allotment for dehumidification and regeneration, the process and regeneration air flowrates are generally identical as can be observed for *StV*, *StR*, *2SD*, and *2SD-IC* (Table 1). For *ICD*, however, due to the lower moisture holding capacity of the regeneration air at low regeneration temperature and higher relative humidity, regeneration air flowrate must be 2.34 times that of the process air (Fig. 4). For *StR*, recirculation of the colder and drier return room air while limiting the extended increase in desiccant temperature allows for a lower regeneration temperature. This approach, however, also limits the specific enthalpy reduction and hence must operate at

much higher flowrate for both the process and regeneration sides to realize the required cooling capacity. These characteristics are major determinants in the many of the evaluation criteria in the following sections.

### 3.2 Regeneration temperature

The effect of employing various strategies to lower regeneration temperature can be seen in the psychrometric plots in Figs. 2, 3, 4, 5 and 6 and summarized in Table 1. *StV* required the highest regeneration temperature at 77.1 °C. In *2SD*, regeneration temperature was brought down to 60.3 °C by dividing dehumidification into two stages and further down to 55 °C when interstage cooling is employed. In *StR*, recirculation of room air can lower the regeneration temperature to 48.3 °C at the expense of increased flowrate. In *ICD*, heat rejection by internal cooling can reduce the regeneration temperature to a very low level depending on the temperature of the coolant and how much heat can be removed. In this case, a conservative regeneration temperature of 45 °C was assumed.

### 3.3 Moisture removal capacity

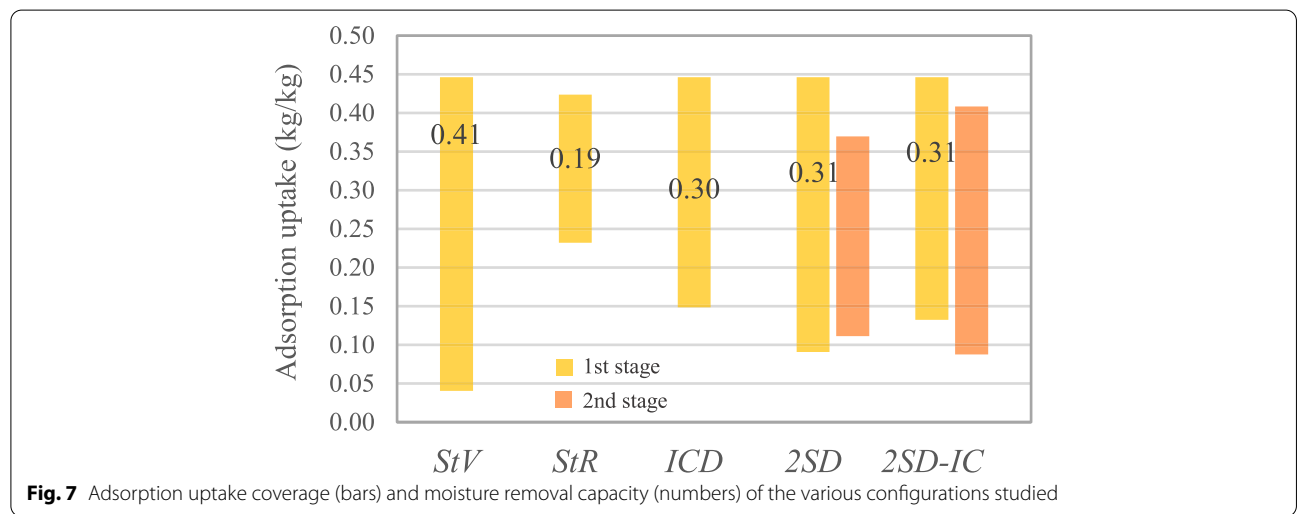
The adsorption uptake coverage and adsorption capacities of the desiccant at their respective operating conditions are shown in Fig. 7. The initial moisture content of the desiccant is defined by the relative humidity of the regeneration air. The high regeneration temperature in *StR* significantly lowers the relative humidity of the desiccant after regeneration consequently allowing more room for moisture adsorption during dehumidification. As regeneration temperature decreases and relative humidity increases, the initial moisture content of the desiccant also increases, thereby limiting the room for additional moisture adsorption. The adsorption capacity of the desiccant reflects the amount of adsorbable moisture per cycle of dehumidification. A low adsorption capacity denotes that the desiccant gets saturated more quickly and hence must be regenerated more frequently. A high regeneration frequency increases heat carryover from regeneration to dehumidification and negatively affects the heat balance in the desiccant system [29, 30].

### 3.4 Thermal COP

Thermal COP describes the amount of cooling output obtained per heat input and can be visually depicted as the  $q_{output}$  and  $q_{input}$ , respectively, in Figs. 2, 3, 4, 5 and 6. Figure 8 summarizes the heating load, while Fig. 9

**Table 3** Dimensions of the components of the DAC systems

Configuration	Desiccant wheel			DPEC				Plate-fin heat exchanger			
	No. of units	Diameter m	Length m	No. of units	Height m	Width m	Length m	No. of units	Height m	Width m	Length m
<i>StV</i>	1	0.405	0.300	1	0.328	0.360	0.614	1	0.358	0.358	0.323
<i>StR</i>	1	0.816	0.091	1	0.683	0.760	0.569	0			
<i>ICD</i>	1	0.395	0.300	1	0.324	0.360	0.397	1	0.347	0.347	0.423
<i>2SD</i>	2	0.400	0.187	1	0.334	0.360	0.704	1	0.354	0.354	0.330
<i>2SD-IC</i>	2	0.395	0.113	1	0.325	0.360	0.484	2	0.355	0.355	0.321
		0.399	0.148						0.351	0.351	0.333
		0.396	0.152								



compares the thermal COP, along with electrical COP, and total COP. It can be observed that *StV* has the lowest heating load, hence giving the highest COPT of 2.24 followed by *2SD-IC* at 2.06. The high COPT of *StV* can be attributed to the effect of heat recovery which minimizes the heating load, whereas the slightly lower COPT for *2SD-IC* is mainly due to the exergy destruction associated with intercooling, thereby increasing the heating load. In *2SD*, heat recovery was performed only once despite having two stages of dehumidification. In effect, additional heating and cooling were necessary for the heat source and DPEC, respectively, hence a slightly lower COPT of 1.42. In *ICD*, heating load is much higher as most of the heat generated during dehumidification is not recovered but rejected to the environment resulting to a reduced COPT of 0.907. In *StR*, the specific heat input becomes greater than the specific enthalpy reduction resulting to a very low COPT of 0.51. The total COP of the DPEC-DAC systems investigated is almost equal to the thermal COP

due to the significantly smaller electrical power requirement (discussion in Section 3.8). This corroborates the assertion of DACs as being a thermally driven cooling system.

### 3.5 DPEC L/H

DPEC L/H describes the dimensionless length required for the DPEC inlet air to be cooled to 20 °C relative to the channel height. For the same target product air temperature, inlet air humidity ratio, and operating conditions, it can be observed from Fig. 10 that the DPEC L/H is directly proportional to the inlet air temperature. Internal cooling for *ICD* and *2SD-IC* effected a lower temperature at the DPEC inlet, thereby lowering DPEC L/H. On the other hand, as the DPEC inlet air comes directly warm from the 2nd stage of dehumidification in *2SD*, a much higher DPEC L/H becomes necessary. It should be noted, however, that as the inlet air temperature increases, the rate of increase in DPEC L/H becomes less. This can be corroborated by the



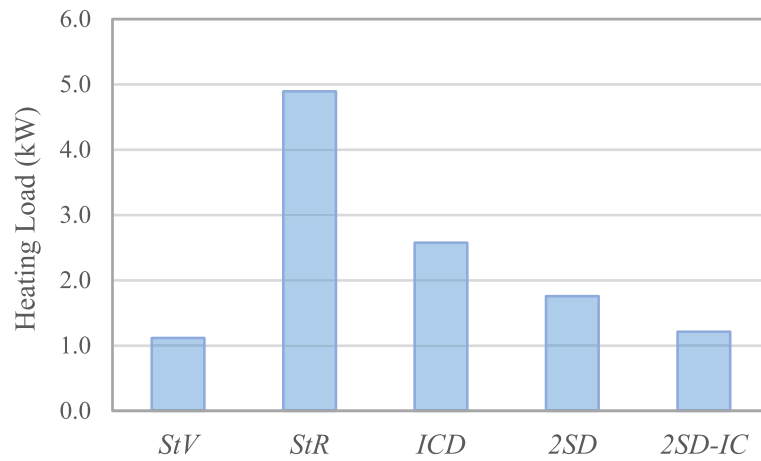


**Fig. 8** Heating load of the various configurations studied

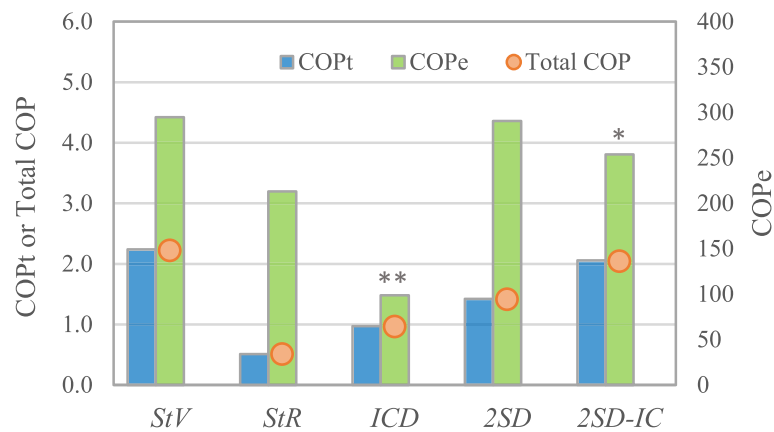


**Fig. 9** Thermal COP, electrical COP, and total COP of the various configurations studied (additional electrical power for \*\*internal cooling and \*interstage cooling unaccounted for)

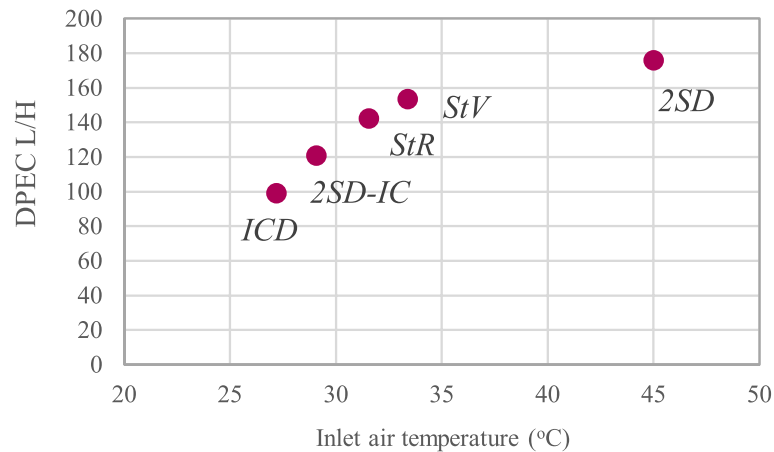


**Fig. 10** DPEC L/H vs inlet air temperature of the five configurations at fixed humidity ratio of 0.010 kg/kg da

increase in dew point effectiveness of DPEC with increasing inlet temperature as shown by other studies [31, 32].

### 3.6 Heat exchanger UA

Figure 11 shows the heat exchanger UA which represents the required heat transfer area given a certain overall heat transfer coefficient to compare the design requirement to achieve 80% heat recovery. Despite the difference in the operating temperature ranges for heat exchange, the heat exchanger UA are similar for *StV*, *2SD*, and *2SD-IC* per heat exchanger. However, as *2SD-IC* utilizes two units for heat recovery, its total heat exchanger UA is twice as large. *ICD* has a smaller heat exchanger UA due to the low heat capacity ratio of the process and regeneration airstreams. Meanwhile, for *StR* at steady state, the dehumidified air temperature is lower than the outdoor air temperature; hence, no practical heat exchange can be made.

### 3.7 System size and design geometry

Table 3 and Fig. 12 show the equipment design geometries and space requirement, respectively, for the desiccant wheels, DPECs, and heat exchangers for the configurations studied. Among the DAC components, DPEC requires a relatively larger space. Without considering airflow ducts, *StV* and *2SD* will demand a similar space requirement as the two configurations differ only in desiccant division in terms of design. Despite the absence of a heat exchanger, *StR* will require the largest space, about twice that of *StV*, due to the higher airflow. *ICD* and *2SD-IC* will require a comparatively larger space than *StV* depending on the additional space requirement for intercooling and interstage cooling, respectively. It should be noted that the space requirement for all configurations will increase further as the heat source is integrated into the system which was not accounted for in this study.



Fig. 11 Heat exchanger UA of the various configurations studied

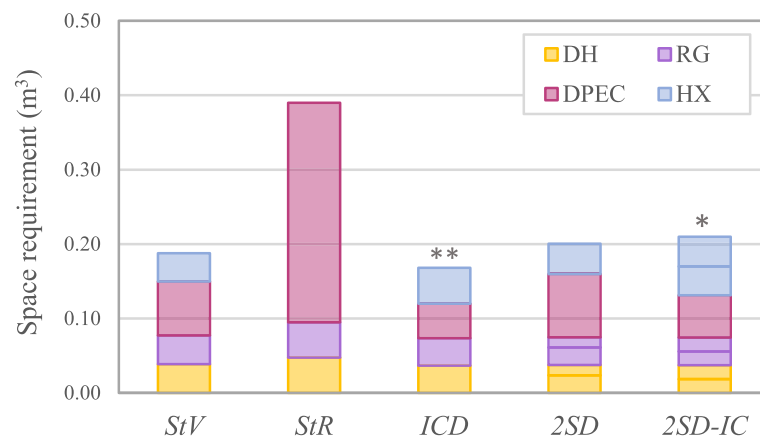


Fig. 12 Overall space requirement of the configurations studied (\*\*internal cooling and \*interstage cooling unaccounted for)

### 3.8 Fan power

As shown in Fig. 13, the smallest fan power requirement, without considering the airflow ducts, is for *StV* and *2SD* due to the simple design. *StR* requires a considerably higher fan power requirement due to the higher mass flow of air. On the other hand, the fan power requirement for *ICD* is several folds larger due to the squared effect of velocity on pressure drop particularly for the regeneration airstream. It should be noted, also, that total power requirement for all configurations may increase further with the integration of the flow ducts and heating system and much further for *ICD* and *2SD-IC* due to internal cooling and intercooling. In terms of electrical power consumption, DAC systems have very high COPE, as shown in Fig. 9, due to the minimal fan power requirement. As a result of the minimal contribution of electricity input to the total energy consumption, the total COP of the system is almost equal to its thermal COP.

### 4 Conclusion

In this study, various configurations of DAC systems based on DPEC were evaluated using seven criteria. Figure 14 summarizes the relative differences of the eight

criteria against *StV*. In this comparison, the inverse of MRC was taken and used instead, to represent the amount of desiccant required per amount of moisture removed, or in the context of a desiccant wheel, is the regeneration frequency or rotational speed, and is hereafter referred to as RF. Similarly, heating load, or the inverse of COPt, was used instead to represent the total amount of sensible heat input required per cooling output. As such, a smaller magnitude for all the seven evaluation criteria are considered more desirable. In this study, the following can be generalized:

1. *StV*, the most common and simple among all the configurations, provide the lowest heating load and the lowest fan power and space requirement but require the highest regeneration temperature.
2. Recirculation of return room air (*StR*) can provide the same cooling capacity and cold air temperature at significantly lower regeneration temperature at a higher air flowrate. This results to a larger equipment size, higher regeneration frequency, and significantly higher heating load.

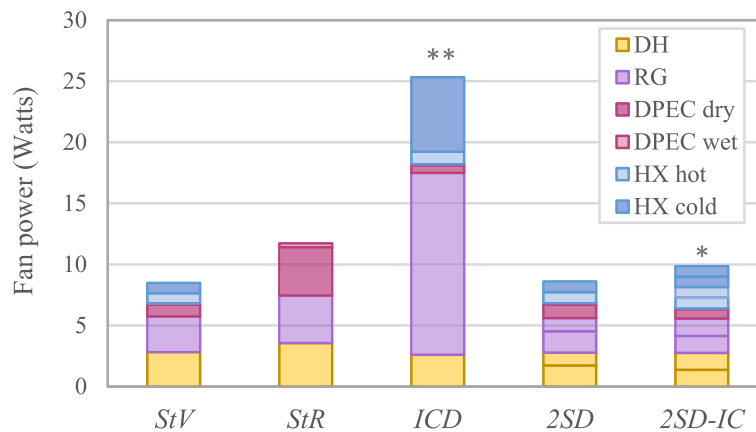


Fig. 13 Fan power requirement of the configurations studied (\*\*internal cooling and \*interstage cooling unaccounted for)

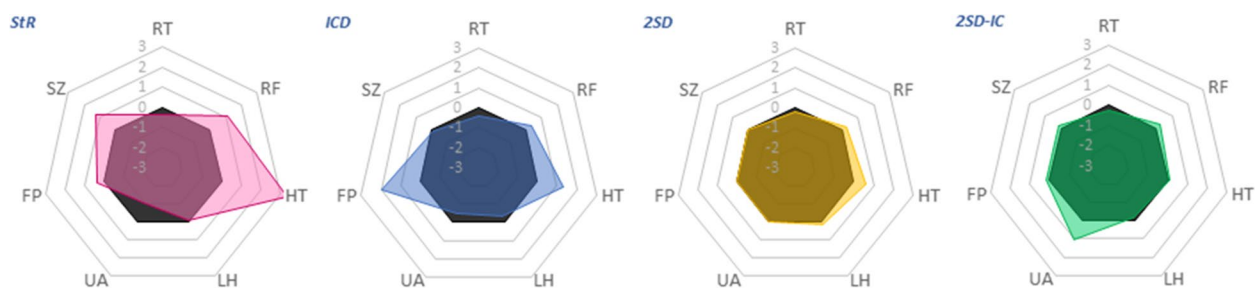


Fig. 14 Relative difference plot of the evaluation criteria against the standard cycle in ventilation mode or *StV* (RT, regeneration temperature; RF, regeneration frequency; HT, heating load; LH-DPEC L/H, UA-heat exchanger UA; FP, fan power; SZ, system size)

3. In a DAC with internally cooled dehumidification (*ICD*), regeneration temperature, DPEC L/H, and heat exchanger UA can be lowered significantly. However, the imbalance between the specific moisture removed during dehumidification and the specific moisture removal capacity of the regeneration air results to an increased air flow requirement for regeneration consequently increasing the fan power requirement quadratically. In addition, higher heating loads are required as a significant amount of the heat generated during dehumidification is not recovered but rejected to the environment.
4. Two-stage dehumidification without intercooling (*2SD*) performs similar to an *StV* at lower regeneration temperature but at the expense of additional heating load and slightly higher DPEC L/H and regeneration frequency.
5. Two-stage dehumidification with intercooling (*2SD-IC*) can reduce regeneration temperature and DPEC L/H with the addition of an intercooler and a second heat exchanger. This system also entails a slightly higher heating load, fan power, regeneration frequency, and space requirement.

Among the criteria evaluated, DPEC L/H and heat exchanger UA are factors that affect capital cost, while heating load, fan power, and regeneration frequency mainly affect operating cost. The overall system size, while affecting capital cost, may also limit the extent of application of the technology as well as consumer acceptance. Regeneration temperature is a limiting factor which depends on the quality of the heat source available which may also affect capital and operating costs. Regeneration heat may be sourced from electric heating, combustion, waste heat, district heating, solar heat, or heat pumps. The accessibility and availability of these resources may vary temporally with location and climate, and hence, one heat source may be preferred over the other. This study can be used as a guide for the selection of a suitable DAC configuration for space cooling based on the objective criteria and the resources available.

## 5 Nomenclature

### Symbols

$C_p$	Isobaric-specific heat, kJ/kg
$D_{wa}$	Water-air diffusion coefficient, $m^2/s$
$d_h$	Hydraulic diameter
$E$	Characteristic energy of adsorption, J/mol
$f$	Friction factor
$H$	Height, m

$h$	Enthalpy, kJ/kg-K
$h_{vap}$	Latent heat of vaporization, kJ/kg
$k$	Thermal conductivity, W/m-K
$L$	Length, m
$m$	Mass, kg
$Nu$	Nusselt number
$P$	Pressure, kPa
$P_v$	Vapor pressure, kPa
$Pr$	Prandtl number
$Q$	Heat input or output, kJ
$q$	Specific heat input or output, kJ/kg da
$r$	DPEC working ratio
$R$	Gas constant, J/mol-K
$T$	Temperature, °C
$u$	Velocity, m/s
$V$	Volumetric flowrate, $m^3/s$
$W$	Humidity ratio, kg/kg dry air
$w$	Adsorption uptake, kg $H_2O$ /kg adsorbent
$z$	Channel height

### Greek letters

$\alpha$	Ratio of channel height to channel width
$\delta$	Combined thickness of plate and water film in DPEC, m
$\zeta$	Loss coefficient
$\eta$	Efficiency
$\nu$	Kinematic viscosity, $m^2/s$
$\rho$	Air density, $kg/m^3$
$\rho_v$	Vapor density, $kg/m^3$

### Subscripts

1/2	Half
a	Air
dp	Dew point
ex	Exhaust
in	Inlet
p	Process
r	Regeneration
s	Saturation
v	Vapor
vap	Vaporization
w	Water

### Abbreviations

*2SD*: Two-stage dehumidification; *2SD-IC*: Two-stage dehumidification with interstage cooling; AC: Air-conditioning; DAC: Desiccant air-conditioning; DEC: Direct evaporative cooling; DH: Dehumidification; DPEC: Dew point evaporating cooling/cooler; COPE: Electrical coefficient of performance; COPT: Thermal coefficient of performance; FP: Fan power; HT: Heating/heater; HX: Heat exchanger; *ICD*: Internally cooled dehumidification; MRC: Moisture removal capacity; NTU: Number of transfer units; *oa*: Outdoor air; *pa*: Product air; *ra*: Return air; RG: Regeneration; *StR*: Standard cycle in recirculation mode; *StV*: Standard cycle in ventilation mode.

### Acknowledgements

The authors would like to acknowledge the Philippine Atmospheric, Geophysical and Astronomical Services Administration (PAGASA) of the Department of Science and Technology of the Philippines for the climate data.

### Authors' contributions

Conceptualization — ML, FM, KT, JL, and TM; investigation — ML; validation, FM, JL, KT, and TM; writing of original draft — ML; review and editing — FM, JL, KT, and TM; supervision — KT and TM. All authors have read and agreed to the published version of the manuscript (ML, Marco Lao; J, Jie Lin; FM, František Mikšík; KT, Kyaw Thu; TM, Takahiko Miyazaki).

### Funding

This study was funded by the Science Education Institute of the Department of Science and Technology (DOST-SEI) of the Philippines.

### Availability of data and materials

The datasets generated during the current study are available at <https://doi.org/10.6084/m9.figshare.21019012>.

### Declarations

#### Competing interests

The authors declare that they have no competing interests.

#### Author details

<sup>1</sup>Department of Energy and Environmental Engineering, Interdisciplinary Graduate School of Engineering Sciences, Kyushu University, 6-1, Kasuga-koen, Kasuga, Fukuoka 816-8580, Japan. <sup>2</sup>Department of Chemical Engineering, University College London, Gower Street, London WC1E 6BT, UK. <sup>3</sup>Research Center for Next Generation Refrigerant Properties (NEXT-RP), International Institute of Carbon-Neutral Energy Research (WPI-I2CNER), Kyushu University, 744 Motoooka, Nishi Ward, Fukuoka 819-0385, Japan.

Received: 18 July 2022 Accepted: 29 August 2022

Published online: 30 September 2022

### References

- ASHRAE, 2007 ASHRAE Handbook: heating, ventilating, and air-conditioning applications: American Society of Heating Refrigerating and Air-Conditioning Engineers. American Society of Heating, Refrigeration and Air-Conditioning Engineers, Inc., Atlanta, 2007.
- D. of E. (Philippines), "Compendium of Philippine Energy Statistics and Information," 2016. [Online]. Available: [https://www.doe.gov.ph/sites/default/files/pdf\\_energy\\_statistics/doe\\_compendium\\_energy\\_statistics.pdf](https://www.doe.gov.ph/sites/default/files/pdf_energy_statistics/doe_compendium_energy_statistics.pdf)
- International Energy Agency (IEA), "Southeast Asia Energy Outlook 2019 – Analysis," 2019. [Online]. Available: <https://www.iea.org/reports/south-east-asia-energy-outlook-2019#>
- International Energy Agency (IEA), "The future of cooling in Southeast Asia," 2019. [Online]. Available: <https://www.iea.org/reports/the-future-of-cooling-in-southeast-asia>
- Jain, S., Dhar, P. L., & Kaushik, S. C. (1995). Evaluation of solid-desiccant-based evaporative cooling cycles for typical hot and humid climates. *International Journal of Refrigeration*, 18(5), 287–296. [https://doi.org/10.1016/0140-7007\(95\)00016-5](https://doi.org/10.1016/0140-7007(95)00016-5)
- Kang, T. S., & Maclaine-Cross, I. L. (1989). High performance, solid desiccant open cooling cycles. *J. Sol. Energy Eng. Trans. ASME*, 111(2), 176–183. <https://doi.org/10.1115/1.3268304>
- Jani, D. B., Mishra, M., & Sahoo, P. K. (2016). "Solid desiccant air conditioning – A state of the art review," *Renew. Sustain. Energy Review*, 60, 1451–1469. <https://doi.org/10.1016/j.rser.2016.03.031>
- La, D., Dai, Y. J., Li, Y., Wang, R. Z., & Ge, T. S. (2010). Technical development of rotary desiccant dehumidification and air conditioning: A review, 14, 130–147. <https://doi.org/10.1016/j.rser.2009.07.016>
- Enteria, N., Yoshino, H., & Sataki, A. (2016). Exergoenvironmental evaluation of the desiccant air-conditioning system subjected to different regeneration temperatures. *Int. J. Air-Conditioning Refrig.*, 24(4), 1–15. <https://doi.org/10.1142/S2010132516500231>
- Miyazaki, T., Nikai, I., & Akisawa, A. (2011). Simulation analysis of an open-cycle adsorption air conditioning system-numeral modeling of a fixed bed dehumidification unit and the maisotsenko cycle cooling unit. *Int. J. Energy a Clean Environ.*, 12(2–4), 341–354. <https://doi.org/10.1615/InterJEnerCleanEnv.2012005977>
- Gadalla, M., & Saghafifar, M. (2016). Performance assessment and transient optimization of air precooling in multi-stage solid desiccant air conditioning systems. *Energy Conversion and Management*, 119, 187–202. <https://doi.org/10.1016/j.enconman.2016.04.018>
- M. Kashif Shahzad, M. Ali, N. Ahmed Sheikh, G. Qadar Chaudhary, M. Shahid Khalil, and T. U. Rashid, "Experimental evaluation of a solid desiccant system integrated with cross flow Maisotsenko cycle evaporative cooler," *Applied Thermal Engineering*, vol. 128, pp. 1476–1487, 2018, doi: <https://doi.org/10.1016/j.applthermaleng.2017.09.105>.
- Sultan, M., El-Sharkawy, I. I., Miyazaki, T., Saha, B. B., & Koyama, S. (2015). An overview of solid desiccant dehumidification and air conditioning systems. *Renewable and Sustainable Energy Reviews*, 46, 16–29. <https://doi.org/10.1016/j.rser.2015.02.038>
- Lin, J., Thu, K., Bui, T. D., Wang, R. Z., Ng, K. C., & Chua, K. J. (2016). Study on dew point evaporative cooling system with counter-flow configuration. *Energy Conversion and Management*, 109, 153–165. <https://doi.org/10.1016/j.enconman.2015.11.059>
- Zhan, C., Duan, Z., Zhao, X., Smith, S., Jin, H., & Riffat, S. (2011). Comparative study of the performance of the M-cycle counter-flow and cross-flow heat exchangers for indirect evaporative cooling - Paving the path toward sustainable cooling of buildings. *Energy*, 36(12), 6790–6805. <https://doi.org/10.1016/j.energy.2011.10.019>
- Mahmood, M. H., Sultan, M., Miyazaki, T., Koyama, S., & Maisotsenko, V. S. (2016). Overview of the Maisotsenko cycle – A way towards dew point evaporative cooling. *Renewable and Sustainable Energy Reviews*, 66, 537–555. <https://doi.org/10.1016/j.rser.2016.08.022>
- Narayanan, R., Saman, W. Y., & White, S. D. (2013). A non-adiabatic desiccant wheel: Modeling and experimental validation. *Applied Thermal Engineering*, 61(2), 178–185. <https://doi.org/10.1016/j.applthermaleng.2013.07.007>
- Zhou, X., Goldsworthy, M., & Sproul, A. (2018). Performance investigation of an internally cooled desiccant wheel. *Applied Energy*, 224(May), 382–397. <https://doi.org/10.1016/j.apenergy.2018.05.011>
- X. Zhou and R. Reece, "Experimental investigation for a non-adiabatic desiccant wheel with a concentric structure at low regeneration temperatures," vol. 201, no. September, 2019.
- Elzahby, A. M., Kabeel, A. E., Bassuoni, M. M., & Abdelgaied, M. (2014). A mathematical model for predicting the performance of the solar energy assisted hybrid air conditioning system, with one-rotor six-stage rotary desiccant cooling system. *Energy Conversion and Management*, 77, 129–142. <https://doi.org/10.1016/j.enconman.2013.08.052>
- Ge, T. S., Li, Y., Wang, R. Z., & Dai, Y. J. (2009). Experimental study on a two-stage rotary desiccant cooling system. *International Journal of Refrigeration*, 32(3), 498–508. <https://doi.org/10.1016/j.ijrefrig.2008.07.001>
- Huan, Z., & Niu, J. (1999). A two-stage desiccant cooling system using low-temperature heat. *Building Services Engineering Research and Technology*, 20(2), 51–55.
- Bourdoukan, P., Wurtz, E., & Joubert, P. (2010). Comparison between the conventional and recirculation modes in desiccant cooling cycles and deriving critical efficiencies of components. *Energy*, 35(2), 1057–1067. <https://doi.org/10.1016/j.energy.2009.06.021>
- Yamaguchi, S., & Saito, K. (2013). Numerical and experimental performance analysis of rotary desiccant wheels. *International Journal of Heat and Mass Transfer*, 60, 51–60. <https://doi.org/10.1016/j.ijheatmasstransfer.2012.12.036>
- Hesselgreaves, J. E., Law, R., & Reay, D. A. (2017). *Compact Heat Exchangers Selection, Design and Operation*. Second.
- Mohammed, R. H., Mesalhy, O., Elsayed, M. L., & Su, M. (2017). Revisiting the adsorption equilibrium equations of silica gel / water for adsorption cooling applications Revisiting the adsorption equilibrium equations of silica gel / water for adsorption cooling applications. *International Journal of Refrigeration*, 86(November), 40–47. <https://doi.org/10.1016/j.ijrefrig.2017.10.038>
- Lin, J., Wang, R. Z., Kumja, M., Bui, T. D., & Chua, K. J. (2017). Multivariate scaling and dimensional analysis of the counter-flow dew point evaporative cooler, 150, 172–187. <https://doi.org/10.1016/j.enconman.2017.08.003>

28. Moshari, S., & Heidarinejad, G. (2017). Analytical estimation of pressure drop in indirect evaporative coolers for power reduction. *Energy and Buildings*, 150, 149–162. <https://doi.org/10.1016/j.enbuild.2017.05.080>
29. M. Goldsworthy and S. White, "The performance of desiccant wheels for desiccant air-conditioning," in *Desiccant-assisted cooling: Fundamentals and applications*, 2014. doi: <https://doi.org/10.1007/978-1-4471-5565-2>.
30. Khan, A. Y. (1998). Cooling and dehumidification performance analysis of internally-cooled liquid desiccant absorbers. *Applied Thermal Engineering*, 18(5), 265–281. [https://doi.org/10.1016/S1359-4311\(97\)00074-4](https://doi.org/10.1016/S1359-4311(97)00074-4)
31. Riangvilaikul, B., & Kumar, S. (2010). An experimental study of a novel dew point evaporative cooling system. *Energy and Buildings*, 42(5), 637–644. <https://doi.org/10.1016/j.enbuild.2009.10.034>
32. Duan, Z., Zhao, X., & Li, J. (2017). Design, fabrication and performance evaluation of a compact regenerative evaporative cooler: Towards low energy cooling for buildings. *Energy*, 140, 506–519. <https://doi.org/10.1016/j.energy.2017.08.110>

### **Publisher's Note**

Springer Nature remains neutral with regard to jurisdictional claims in published maps and institutional affiliations.